PARAMETERS CALIBRATION OF DISCRETE ELEMENT MODEL FOR CRUSHED CORN STALKS
/
碎玉米秸秆离散元模型参数标定

Min FU*, Xiaoqing CHEN, Zefei GAO, Chengmeng WANG, Bing XU, Yilin HAO[1]
Northeast Forestry University, College of Mechanical and Electrical Engineering, Harbin / China
Tel: +86 15663688203; E-mail: fumin1996@163.com
DOI: https://doi.org/10.35633/inmateh-69-37

Keywords: *crushed corn stalk, angle of repose, discrete element simulation, parameter calibration*

ABSTRACT
For the problem of lacking reliable parameters during simulation analysis of the crushed corn stalk (CCS) micro-comminution process with gas-solid coupling method, the simulation parameters are calibrated using a combination of physical measurements and virtual experiments with CCS as the research object. The intrinsic parameters of CCS are obtained by physical experiment, and the stacking test is carried out by cylinder lifting method, and the actual angle of repose(AoR) is obtained as 44.12° by fitting the boundary line with Matlab software; the discrete element model of CCS is established, and the virtual stacking test is carried out by EDEM software; CCS-CCS dynamic friction coefficient, CCS-CCS static friction coefficient and JKR (Johnson-Kendall-Roberts) surface energy are identified as the parameters with significant effects on the AoR by Plackett-Burman test; the steepest climb test is leveraged to determine the center of response surface analysis; the quadratic polynomial regression model of the simulation parameters and the AoR is established by the Box-Behnken test using the AoR as the evaluation index, and the optimal combination of the significant parameters are obtained as follows: the CCS-CCS dynamic friction coefficient is 0.14, the CCS-CCS static friction coefficient is 0.55, and the JKR surface energy is 0.12; the AoR verification test is conducted based on the optimal combination of the significant parameters. The results show that the AoR of the CCS is 43.82°, which is 0.68% of the actual AoR, indicating that the parameter combination is reliable. The data obtained in this research can provide corresponding simulation parameters for CCS discrete element simulation and the development of straw micro-crushing equipment.

摘要
针对采用气固耦合法对碎玉米秸秆微粉碎过程仿真分析时，所需的仿真参数缺乏可靠数值的问题，以碎玉米秸秆为研究对象，采用物理测定与虚拟试验相结合的方法对仿真参数进行标定。通过物理试验获取碎玉米秸秆的本征参数，采用圆筒提升法进行堆积试验，并利用 Matlab 软件拟合边界线得到实际休止角为 44.12°；建立碎玉米秸秆离散元模型，利用 EDEM 软件进行虚拟堆积试验；通过 Plackett-Burman 试验，确定对休止角影响显著的参数为碎玉米秸秆间滚动摩擦因数、碎玉米秸秆间静摩擦因数和 JKR（Johnson-Kendall-Roberts）表面能；利用最陡爬坡试验，确定响应面分析的中心；以休止角为评价指标，通过 Box-Behnken 试验建立显著参数与碎秸秆休止角的二次多项式回归模型，对显著参数的取值进行寻优，得到较优的显著参数组合为：碎玉米秸秆间滚动摩擦因数为 0.14、碎玉米秸秆间静摩擦因数为 0.55、JKR 表面能为 0.12；基于最优参数组合进行休止角验证试验，试验结果表明，该参数组合下碎玉米秸秆的休止角为43.82°，与实际休止角误差为0.68%，表明该参数组合具有可靠性。本文得到的数据可为碎玉米秸秆离散元仿真以及秸秆微粉碎设备的研发提供相应的仿真参数。

INTRODUCTION
Corn stalk can be used as a new energy saving and environmental protection raw material after micro-grinding to achieve fine and high value utilization, so that it is no longer limited to low value-added fields such as heating and feeding, and could also save resources and protect the environment (*Koul et al., 2021*). At present, stalk powder is used in many fields such as composite materials, biodegradable plastics, hydrogen production and battery materials, and with increasing market demand. (*Mustafa* et *al., 2022; Cindradewi et al., 2021; Gao et al., 2022; Nita et al., 2021*). But existing stalk micro-crushing equipment can hardly support the demand of stalk powder scale up and industrialization.

---

[1] *Min Fu, Prof.; Xiaoqing Chen, M.S.Stud.Eng; Zefei Gao, M.S.Stud.Eng; Chengmeng Wang, M.S.Stud.Eng; Bing Xu, M.S.Stud.Eng; Yilin Hao, M.S. Stud.Eng.*

It is necessary to research and develop the micro-crushing equipment. The movement process of stalk powder is studied by using DEM, and further the grinding mechanism of straw is studied, which provides a new idea for the research of micro-crushing equipment.

In order to improve the accuracy of simulation test, many scholars have calibrated discrete element parameters of different materials based on Angle of repose (AoR) test. *Mu et al., (2021),* studied the discrete element model parameters of the stem and leaf of smashed sweet potatoes by combining physical experiments and virtual calibration. *Huan et al., (2022*), measured the intrinsic parameters of king grass stalks by physical experiments, using the index of AoR, the discrete element parameters of king grass stalks were calibrated using response surface optimization method, and the calibration results were verified by throwing trajectory tests; *Wang et al., (2021),* conducted parameter calibration tests using straw powder as homogeneous material in the mechanical properties test of corn straw powder. However, there is no study on calibration for discrete element parameterization of the crushed corn stalk (CCS). In this paper, the range of CCS characteristic parameters, CCS-CCS and CCS-65Mn steel plate (65Mn SP) contact parameters are measured by physical experiments, and a multisphere model of CCS is created based on EDEM software. By means of the actual AoR measured by stacking test, using the Plackett-Burman test, the steepest climb test and the Box-Behnken test, the discrete element model of CCS is calibrated to obtain the parameters of CCS which could be used in discrete element simulation. It is supposed to provide reliable discrete element basic parameters for the research and development simulation of straw micro-grinding equipment.

MATERIALS AND METHODS

Test material

The experimental materials are obtained from Donghai County, Lianyungang City, Jiangsu Province, China. The corn stalks are crushed using a Konnon straw crusher, and the crushed corn stalks (CCS) are sieved through a 20-mesh screen using a ZFJ-Ⅱ standard inspection sifter. The average length of the CCS is 10 mm and the diameter is 4 mm measured by the vernier caliper, and the moisture content of the CCS is 11.63% evaluated by rapid moisture tester.

CCS feature parameter measurement

Since the shape of CCS varies in size, the overflow method is leveraged to measure the volume of CCS (*Mu et al.,2021*). The paper cup is filled with pure water and put into the sink, 5g of CCS is weighed using a high-precision electronic scale (error ±0.05g), and the weighed CCS is put into the paper cup, then the pure water will overflow. Because the density of CCS is smaller than water, therefore, pressure the cover plate on the paper cup, so that the CCS is submerged in water, as shown in Figure 1.

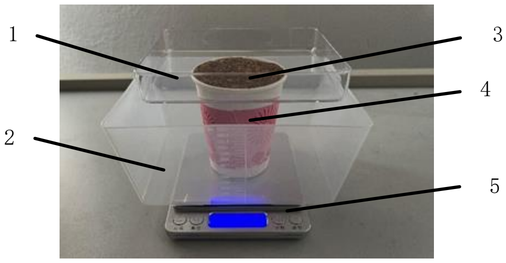

Fig. 1 - Measurement of CCS density

1-Cover plate; 2-Sink; 3-CCS; 4-Paper cup; 5-Electronic scale;

When the water no longer overflows, the paper cup will be removed from the sink. At this time, the volume of overflowing water is known as the volume of CCS. The obtained value is substituted into formula (1), and the density of CCS can be obtained.

$$\rho = \frac{m}{v} \tag{1}$$

where: ρ - density of CCS, kg/m^3;

m - mass of CCS，kg;

v – volume of CCS, m^3.

Repeating the above operations five times, the density of CCS is obtained as: 116.15 kg/m^3, 126.14 kg/m^3, 101.42 kg/m^3, 112.35 kg/m^3, 115.74 kg/m^3, with an average density of 114.36 kg/m^3.

The stalk compression test is carried out using the universal testing machine (WDW-100 type, China Changchun Kexin test apparatus Co., Ltd. production, see Figure 2), with the test loading speed of 5 mm/min. According to the change of straw diameter and height after the test, the shear modulus of stalk is obtained as 2.5 MPa, Poisson's ratio as 0.3. The relationship between shear modulus, elastic modulus and Poisson's ratio is shown in Equation 2.

$$G = \frac{E}{2(1+\mu)} \tag{2}$$

where: μ - Poisson's ratio;
E - Elastic modulus, GPa;
G - Shear modulus, MPa.

Fig. 2 - Radial global compression test of CCS
1-CCS; 2- WDW-100 universal tester; 3- Indenter;

Since 65Mn is commonly used as cutting tool material in straw micro-crushing equipment, 65Mn is selected as the test steel. The sliding method is used to measure the static friction coefficient of CCS-CCS and CCS-65Mn SP. The experimental apparatus consists of an angle digital display instrument and homemade test bench (see Figure 3). When the test begins, the digital display inclinometer and 65Mn SP are fastened horizontally on the test bench. Because the rolling of CCS will increase the test error, the CCS is glued together and placed on the steel plate. One end of the test bench is slowly lifted, when the first CCS particle begins to slide, stop lifting at the same time, and record the value on the inclinometer (*Huan et al., 2022; Fang et al., 2022*).

The above operations are repeated 10 times and the values of the inclination angle are between 21° and 35°. The CCS-65Mn SP static friction coefficient ranges from 0.4 to 0.7 by substituting the values into formula (3).

$$\mu = \tan\alpha \tag{3}$$

where: μ - static friction coefficient;
α - inclination angle.

Fig. 3 -Static friction coefficient measurement device
1-Angle digital display instrument; 2-CCS; 3-homemade test stand; 4-65Mn SP;

The inclined plane method is also used to measure the CCS-CCS static friction coefficient. Because the shape of the CCS is irregular, it is difficult to directly measure the static friction coefficient between the CCS, so the CCS is laid flat on the steel plate to form a material board, and then the CCS is placed on the material board. One end of the test stand is slowly lifted, when the first CCS particle begins to slide, stop lifting and record the value on the inclinometer. The above operations are repeated 10 times and the values of the inclination angle are between 20° and 37°. The values are substituted into formula 3 to obtain the CCS-CCS static friction coefficient in the range of 0.35~0.75. Based on the preliminary experimental measurements and review of relevant literature, the range of values for the parameters of AoR simulation model for CCS is determined, as illustrated in Table 1 (*Zhang et al., 2018; Song et al., 2022*).

Table 1

Parameters of AoR simulation model for CCS

Parameters	Numerical value
Poisson's ratio of CCS x_1	0.2~0.4
Shear modulus of CCS G_1 / MPa	2.5
CCS density ρ_1 /(kg·m^{-3})	114.36
Poisson's ratio of 65Mn SP v_2	0.3
Shear modulus of 65Mn SP G_2 / MPa	79000
65Mn SP density ρ_2 / (kg·m^{-3})	7865
CCS-CCS Coefficient of restitution x_2	0.2~0.4
CCS-CCS static friction coefficient x_3	0.35~0.75
CCS-CCS dynamic friction coefficient x_4	0.03~0.15
CCS-65Mn SP Coefficient of restitution x_5	0.3~0.6
CCS-65Mn SP static friction coefficient x_6	0.4~0.7
CCS-65Mn SP dynamic friction coefficient x_7	0.01~0.3
CCS-CCS JKR surface energy x_8 /(J·m^{-2})	0.04~0.12

Physical test on the AoR of CCS

The cylinder lifting method is used to calculate the AoR of the CCS (*Jia et al., 2021*). The material's size determines the size of the cylinder, which has a diameter more than four to five times the material's maximum length and a height to diameter ratio of three to one (*Zhang et al., 2022*). Because the average length of the CCS is 10 mm, the diameter of the cylinder used in this test is 50 mm, the height is 150 mm, and the size of the test steel plate is 300×300×5 mm. The CCS screened by ZFJ-II standard inspection screening machine is used as the test material. After the cylinder is placed vertically on the 65Mn SP, the CCS is filled with the cylinder, and the cylinder is constantly lifted at the speed of 0.05 m/s using WDW-100 universal testing machine, and the CCS will form a pile on the 65Mn SP through the bottom of the cylinder, as shown in Figure 4. A vertical picture of the front of the CCS pile is photographed by a camera after the straw pile is stable.

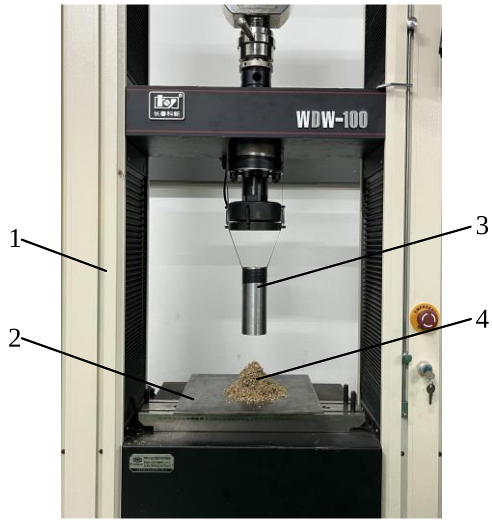

Fig. 4 - AoR physical test

1-WDW-100 universal tester; 2-65Mn SP; 3-Cylinder; 4-CCS pile

The frontal image is successively processed by grayscale processing, binarization processing and edge contour extraction by using Matlab software (see Figure 5), and then linear fitting is carried out on the edge contour, and the slope obtained by linear fitting is read, so as to obtain the AoR of the frontal image (*Chen et al., 2022*). The above steps are retested 5 times, and the test results are exhibited in Table 2.

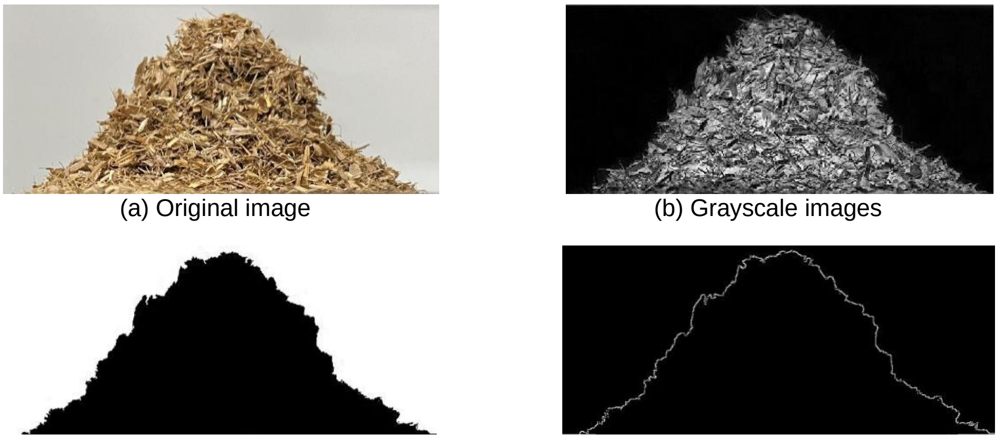

(a) Original image (b) Grayscale images

(c) Binarized images (d) Edge contour

Fig. 5 – AoR image processing

Table 2

AoR measurement

Number	AoR θ / (°)
1	44.62
2	45.21
3	46.09
4	41.89
5	42.77
average value	44.12

Establishment of the simulation model

Contact model selection

The commonly used Hertz-Mindlin contact model only calculates the elastic deformation of the material without considering the adhesive force between the materials (*Qu et al., 2020*). The Hertz-Mindlin with JKR contact model considers the adhesion force-JKR (Johnson-Kendall-Roberts) on the basis of Hertz theory. JKR can reflect the adhesion force between materials, and the influence of adhesion force on material motion can be obtained by calculation (*Wang et al., 2022; Tian et al., 2021; Dong et al., 2022*). Since the CCS has a certain bonding property, Hertz-Mindlin with JKR contact model is chosen for simulation calculation. The magnitude of the normal elastic force in the model is based on the normal overlap and surface energy, and the calculation equation is:

$$F_{JKR} = -4\sqrt{\pi\gamma E^*}\alpha^{\frac{3}{2}} + \frac{4E^*}{3R^*}\alpha^3 \tag{4}$$

$$\delta = \frac{\alpha^2}{R^*} - \sqrt{\frac{4\pi\gamma\alpha}{E^*}} \tag{5}$$

There into

$$\frac{1}{E^*} = \frac{1-v_1^2}{E_1} + \frac{1-v_2^2}{E_2} \tag{6}$$

$$\frac{1}{R^*} = \frac{1}{R_1} + \frac{1}{R_2} \tag{7}$$

where: F_{JKR} - JKR normal elastic force, N;

E^*- Equivalent modulus of elasticity, Pa;

δ - Normal overlap between two contacting particles, m;

α - Radius of the contact circle between two contacting particles, m;

γ - Surface energy, N/m;

R^* - Equivalent contact radius, m;

R_1, R_2 - Radius of contact of two particles, m;

v_1, v_2 - Poisson's ratio of two contact particles;

E_1, E_2 - Modulus of elasticity of two contact particles, Pa.

Simulation model building

Because of the small diameter of the CCS, multiple particles are needed to form the CCS model, which will increase the computer processing time, so the CCS is simplified into a cylinder with the same size. The average length of the CCS is measured as 10 mm and the diameter as 4 mm using vernier calipers. Then, the model is generated at the same size in EDEM and the geometric model of the CCS is illustrated in Figure 6.

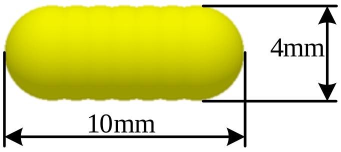

Fig. 6 - Geometric model of CCS

The models of the 65Mn cylinder (used to hold the CCS) and the steel plate are generated in EDEM, the length of the 65Mn cylinder is 150 mm and the diameter is 30 mm, the length and width of the 65Mn SP are both 300 mm.

Simulation of the AoR of CCS

The pellet plant is a circular plane with a diameter of 50 mm, which is dropped from the top of the cylinder, and the radius of the produced pellets is between 0.75 and 1.25 of the prototype radius. Dynamic random generation is used, with a generation rate of 5000 pcs/s and a uniform drop speed of 1m/s and a filling time of 0.6 s. The simulation fixed time step is 20% of the Rayleigh time step and the grid size is 2.5R. After the particles are filled, the cylinder is lifted at a uniform speed of 0.05 m/s and the particles fall on the 65Mn SP by gravity to form a particle pile (*Zhang et al., 2022; Coerzee, et al., 2022;*), as shown in Figure 7, and the AoR of the pile is read by Matlab software after the pile is stabilized.

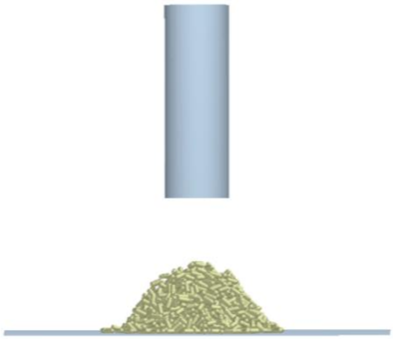

Fig. 7 - Simulation test of AoR

RESULTS

Plackett-Burman screening test and significance analysis

The Plackett-Burman test can be used to screen out the parameters that significantly affect the AoR. In order to simplify the test process, the high-level parameter is set as twice the low-level parameter, as shown in Table 3. Design-expert 8.0.6 software is used to design the experiment, and a total of 12 groups of simulation tests are performed. The testing program and simulation results are shown in Table 4.

Table 3

The parameters of Plackett Burman test

Symbol	Parameters	Level	
		low-level	high-level
x_1	Poisson's ratio of CCS	0.2	0.4
x_2	CCS-CCS restitution coefficient	0.25	0.5
x_3	CCS-CCS static friction coefficient	0.35	0.7
x_4	CCS-CCS dynamic friction coefficient	0.01	0.02
x_5	CCS-65Mn SP restitution coefficient	0.3	0.6
x_6	CCS-65Mn SP static friction coefficient	0.4	0.8
x_7	CCS-65Mn SP dynamic friction coefficient	0.01	0.02
x_8	CCS JKR surface energy / (J·m^{-2})	0.01	0.02

Plackett-Burman Test scheme and results **Table 4**

Number	x_1	x_2	x_3	x_4	x_5	x_6	x_7	x_8	AoR θ / (°)
1	1	1	-1	1	1	1	-1	-1	30.27
2	-1	1	1	-1	1	1	1	-1	27.42
3	1	-1	1	1	-1	1	1	1	37.07
4	-1	1	-1	1	1	-1	1	1	32.23
5	-1	-1	1	-1	1	1	-1	1	31.34
6	-1	-1	-1	1	-1	1	1	-1	28.07
7	1	-1	-1	-1	1	-1	1	1	29.56
8	1	1	-1	-1	-1	1	-1	1	30.34
9	1	1	1	-1	-1	-1	1	-1	28.55
10	-1	1	1	1	-1	-1	-1	1	36.53
11	1	-1	1	1	1	-1	-1	-1	30.55
12	-1	-1	-1	-1	-1	-1	-1	-1	25.54

Design-Expert 8.0.6 is used to analyze the data in Table 4, and the variance analysis of test results is shown in Table 5. As can be seen from Table 5, P=0.0277<0.5 of Plackett-Burman test model indicates that this regression model is significant. The *p*-values of each parameter are ranked and three parameters are found to have *p*<0.5, among which, *p*<0.01 for the CCS-CCS dynamic friction coefficient x_4 and CCS JKR surface energy x_8, which are extremely significant parameters, and p<0.05 for the CCS-CCS static friction coefficient x_3, which are significant parameters. Therefore, the steepest climb test is conducted for x_3, x_4 and x_8.

Table 5

Significance analysis of Plackett-Burman test parameters

Parameters	Sum of squares	df	F-value	p-value	Significance ranking
Model	124.61	8	15.55	0.0227*	
x_1	2.26	1	2.26	0.2302	4
x_2	0.86	1	0.86	0.4225	6
x_3	19.84	1	19.80	0.0211*	3
x_4	40.18	1	40.10	0.0080**	2
x_5	1.87	1	1.87	0.2648	5
x_6	0.20	1	0.20	0.6848	8
x_7	0.23	1	0.23	0.6629	7
x_8	59.116	1	59.04	0.0046**	1

*Note: ** Indicates that the influence is very significant (P<0.01), * the effect is significant (P<0.05).*

Analysis of the steepest climbing test

According to the screening results of the above tests, the steepest climb test is conducted for x_3, x_4 and x_8. The relative error between the actual AoR and the simulation AoR is calculated to determine the optimal range of simulation parameters. The CCS-CCS dynamic friction coefficient is taken as 0.01-0.13, the CCS JKR surface energy is taken as 0.03-0.15, the CCS-CCS static friction coefficient is taken as 0.35-0.75, and the remaining parameters are selected in the middle level for 5 sets of tests, and the test protocol and results are shown in Table 6. Table 6 shows that 4th group of tests has relatively small errors, so the optimal parameter range is around the 4th group of parameter values. Therefore the 4th group of parameter values are taken as the central point of the follow-up test and the 3rd and 5th group of parameter values are used as low level and high level, respectively.

Test design scheme and results of path of steepest ascent method **Table 6**

Number	x_3	x_4	x_8	AoR / (°)	Relative errors φ /%
1	0.35	0.03	0.04	32.43	26.45
2	0.45	0.06	0.06	35.22	20.17
3	0.55	0.09	0.08	37.16	15.78
4	0.65	0.12	0.10	41.91	5.01
5	0.75	0.15	0.12	48.30	9.47

Box-Behnken test analysis

Design-Expert 8.0.6 is used to design the Box-Behnken test, with center point per block adjusted to 3. A total of 15 groups of tests are carried out. The test scheme and results are shown in Table 7. Multiple regression fitting is performed on the test results, and the regression equation of the AoR is obtained as:

$$AoR = 41.77 + 2.43x_3 + 1.48x_4 + 3.18x_8 - 0.69x_3x_4 - 0.40x_3x_8 + 0.19x_4x_8 + 1.25x_3^2 + 0.37x_4^2 - 1.22x_8^2 \quad (9)$$

Table 7

Box-Behnken test scheme and results

Number	x_3	x_4	x_8	AoR θ / (°)
1	-1	-1	0	38.32
2	0	-1	1	42.40
3	0	0	0	41.65
4	-1	0	-1	35.87
5	-1	1	0	43.03
6	0	-1	-1	36.82
7	1	0	1	46.91
8	0	1	1	45.39
9	1	-1	0	45.13
10	-1	0	1	43.42
11	0	1	-1	39.05
12	0	0	0	41.58
13	1	0	-1	40.97
14	0	0	0	42.07
15	1	1	0	47.06

According to the results of variance analysis of the model (see Table 8), the model's p=0.0001, determination coefficient R^2=0.9918, and correction determination coefficient R_{adj}^2=0.9770, both of which are close to 1, indicating that the regression equation fits well. The coefficient of variation is 1.23%, which indicates that the experiment is reliable. The precision (Adeq Precision) is 26.586, which indicates that the model can predict the AoR of CCS better. x_3, x_4, x_8, x_3^2 and x_8^2 have highly significant effects on the AoR of CCS, and x_3x_4 has significant effects on the AoR of CCS.

Table 8

Variance analysis of Box-Behnken quadratic model

Source of variance	Sum of Square	Degree of freedom	Mean Square	p-value
Model	160.92	9	17.88	0.0001**
x_3	47.19	1	47.19	<0.0001**
x_4	17.58	1	17.58	0.0005**
x_8	80.71	1	80.71	<0.0001**
x_3x_4	1.93	1	1.93	0.0432*
x_3x_8	0.65	1	0.65	0.1798
x_4x_8	0.14	1	0.14	0.4949
x_3^2	5.75	1	5.57	0.0056**
x_4^2	0.51	1	0.51	0.2266
x_8^2	5.51	1	5.51	0.0061**
Residual	1.33	5	0.27	
Lack of Fit	1.19	3	0.40	0.1538
Pure Error	0.14	2	0.07	

Based on the results of ANOVA, it can be seen that x_3x_4 interaction terms have a significant effect on the AoR of the CCS, and the corresponding surface of the interaction is plotted using Design-Expert 8.0.6 software in Fig. 8. From Fig. 8, it can be seen that when the value of x_4 is fixed, the AoR increases with the increase of x_3, and the variation tendency is obvious, so x_3 has significant effect on the AoR of CCS.

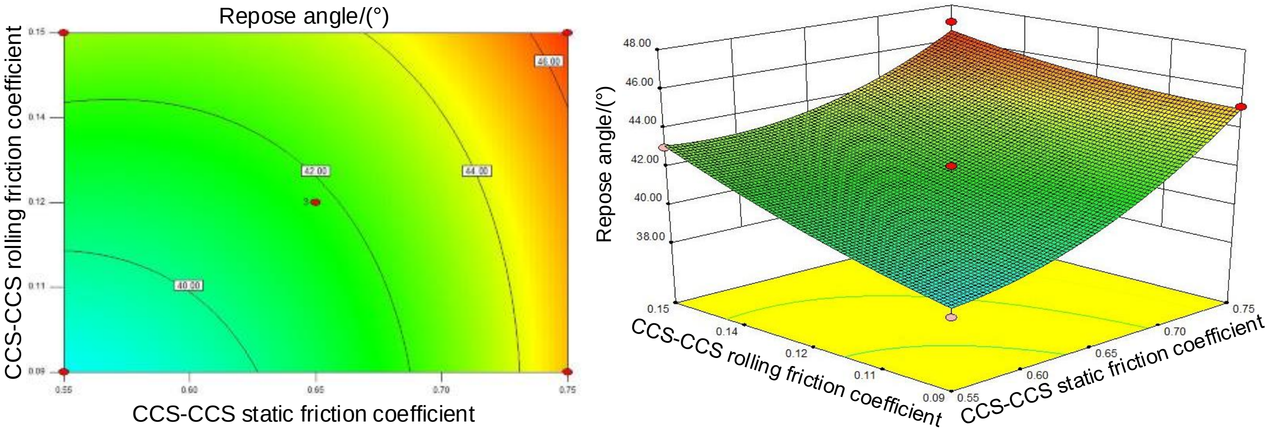

Fig. 8 - Interaction response surface diagrams

Taking the AoR of the physical experiment of CCS as target value, formula (9) is optimized and solved by Design-Expert 8.0.6, and the optimal combination of parameters is obtained as follows: x_3 is 0.55、x_4 is 0.14 and x_8 is 0.12. Other parameters are taken as intermediate values.

In order to verify the accuracy of the above parameters, they are substituted into EDEM for 5 times of simulation tests. The mean value of the measured AoR is 43.82°, and the relative error between the measured AoR and the AoR of physical experiment (44.12°) is 0.68%, which verifies the authenticity and reliability of the simulation test.

(a)Physical tests (b) Simulation test

Fig.9 - Comparison of physical test and simulation test

CONCLUSIONS

The measurement of CCS-related parameters is carried out based on the physical experiment method. The average length of CCS is 10 mm and the diameter is 4 mm using vernier calipers; the moisture content of CCS is 11.63% using a rapid moisture tester; the density of CCS is 114.36 kg/m3 using the overflow method; Through compression test with a universal testing machine, the shear modulus of CCS is 2.5 MPa and Poisson's ratio is 0.3; The range of static friction coefficient of CCS-CCS and CCS-65Mn SP measured by sliding method is 0.35-0.75 and 0.4-0.7 respectively.

According to the stacking test of CCS by cylinder lifting method, a vertical picture of the front of the CCS pile is photographed by camera, and the edge profile of the image is linearly fitted by Matlab software, and the AoR of the CCS pile is obtained as 44.12°. The Hertz-Mindlin with JKR contact model is adopted to establish the simulation model of CCS in EDEM. The model is a cylinder with length of 10 mm and diameter of 4 mm, which is composed of 7 spheres with diameter of 4 mm.

Plackett-Burman test shows that the effects of rolling friction coefficient of CCS-CCS, JKR surface energy and static friction coefficient of CCS on the AoR of CCS are more significant. The simulation parameters of CCS are optimized by taking the AoR of CCS is 44.12° as the test target. According to the results of Box-Behnken test, a set of solutions which are close to the results of physical experiment are obtained: the CCS-CCS static friction coefficient is 0.55, the CCS-CCS rolling friction coefficient is 0.14, and the JKR surface energy is 0.12. According to the simulation parameters obtained, five stacking tests are carried out in EDEM, and the average AoR is obtained as 43.68°, with a relative error of 0.68% compared to the actual experiment results. The calibration results are authentic and trustworthy on the basis of the verification test results, and it can provide basic parameters for the simulation of the mechanized operation of CCS in the stages of micro-crushing and collecting.

ACKNOWLEDGEMENT

This paper was funded by the National Natural Science Foundation of China (Grant No.51975114).

REFERENCES

[1] Chen B., Liu Y., Yu Q.X., Chen X.B., (2022), Calibration of soil discrete element contact parameter in rhizome medicinal materials planting area in hilly region. *INMATEH Agricultural Engineering*, Vol.68, Issue 03, pp.512-532.

[2] Cindradewi A.W., Bandi R., Park C.W., (2021), Preparation and Characterization of Polybutylene Succinate Reinforced with Pure Cellulose Nanofibril and Lignocellulose Nanofibril Using Two-Step Process. *Polymers*, Vol.13, Issue 22, pp.3945-3945.

[3] Coerzee C.J., Scheffler O.C., (2022), Review: The Calibration of DEM Parameters for the Bulk Modelling of Cohesive Materials. *Processes,* Vol.11, Issue 01, pp.5.

[4] Dong X.Q., Zheng H.N., Jia X., Li Y.L., Song J.N., Wang J.C., (2022), Calibration and experiments of the discrete element simulation parameters for rice bud damage. *INMATEH Agricultural Engineering*, Vol.68, Issue 03, pp.659-668.

[5] Fang W.Q., Wang X.Z., Han D.L., Chen X.G., (2022), Review of material parameter calibration method. *Agriculture*, Vol.12, Issue 05, pp.706.

[6] Gao Z.H., Shang S.Q., Xu N., Wang D.W., (2022), Parameter calibration of discrete element simulation model of wheat straw-soil mixture in Huang Huai Hai production area. *INMATEH Agricultural Engineering*, Vol.66, Issue 01, pp.201-210. Romania.

[7] Huan X.L., Wang D.C., You Y., Ma W.P., Zhu L., Li S.B., (2022), Establishment and calibration of discrete element model of king grass stalk based on throwing test. *INMATEH Agricultural Engineering*, Vol.66, Issue 01, pp.19-30.

[8] Jia H., Deng J., Deng Y., (2021), Contact parameter analysis and calibration in discrete element simulation of rice straw. *J. Agric. & Biol. Eng*, Vol.14, Issue.04, pp.72-81.

[9] Koul B., Yakoob M., Shah M.P., (2021), Agricultural waste management strategies for environmental s ustainability. *Environmental Research,* Vol.206, Issue.4, pp.112285.

[10] Mu G.Z., Qi X.T., Zhang W.Z., Lv Z.Q., Zhang T.T., Wang S.W., (2021), Parameter Measurement and Calibration in Discrete Element Simulation of Broken Sweet Potato Seedlings. American Journal of Bio chemistry and Biotechnology, Vol.17, Issue.02, pp.256-266.

[11] Mustafa M.S., Muneer M.A., Zafar M.Q., et al. (2022), Process parameter optimization for Fused Filam ent Fabrication additive manufacturing of PLA/PHA biodegradable polymer blend. *International Polyme r Processing*, Vol.37, Issue.1, pp.1-14.

[12] Nita C., Zhang B., Dentzer J., (2021), Hard carbon derived from coconut shells, walnut shells, and corn silk biomass waste exhibiting high capacity for Na-ion batteries. *Journal of Energy Chemistry*, Vol.58, Issue 07, pp.207-218.

[13] Qu T.M., Feng Y.T., Zhao T.T., Wang M., (2020), A hybrid calibration approach to Hertz−type contact parameters for discrete element models. *International Journal for Numerical and Analytical Methods in Geomechanics*, Vol.44, Issue 09, pp.1281-1300.

[14] Song Z.H., Li H., Yan Y.F., Tian F.Y., (2022), Calibration Method of Contact Characteristic Parameters of Soil in Mulberry Field Based on Unequal-diameter Particles DEM Theory (桑园土壤非等径颗粒离散元仿真模型参数标定与试验). *Transactions of the Chinese Society for Agricultural Machinery*, Vol.53, Issue 06, pp.21-33.

[15] Tian X.L., Cong X., Qi J.T., Guo H., Li M., Fan X.H., (2021), Parameter Calibration of Discrete Element Model for Corn Straw − Soil Mixture in Black Soil Areas (黑土区玉米秸秆-土壤混料离散元模型参数标定). *Transactions of the Chinese Society for Agricultural Machinery*, Vol.52, Issue 10, pp.100-108+242.

[16] Wang W.W., Cai D.Y., Xie J.J., (2021), Parameters calibration of discrete element model for corn stalk powder compression simulation（玉米秸秆粉料致密成型离散元模型参数标定）. *Transactions of the Chinese Society for Agricultural Machinery*, Vol.52, Issue 03, pp.127-134.

[17] Zhang P., Zhang H., Li J.M., Tan C.L., Zhang J.X., (2022), Parametric calibration of cotton straw parameters in Xinjiang based on discrete elements. *INMATEH Agricultural Engineering*, Vol.67(2), pp.314-322.

[18] Zhang T., Liu F., Zhao M.Q., Wang W., (2018), Determination of corn stalk contact parameters and calibration of discrete element method simulation（玉米秸秆接触物理参数测定与离散元仿真标定）. *Journal of China Agricultural University*, Vol.23, Issue.04, pp.120-127.

[19] Zhang W., Wang F., (2022), Parameter calibration of American ginseng seeds for discrete element. *International Journal of Agricultural and Biological Engineering*, Vol.15, Issue 06, pp.16-22.